Formation of Transient Amorphous Calcium Carbonate Precursor in Quail Eggshell Mineralization: An In Vitro Study

ARTICLE *in* BIOMACROMOLECULES · DECEMBER 2006

Impact Factor: 5.75 · DOI: 10.1021/bm0605412 · Source: PubMed

7 AUTHORS, INCLUDING:

Rajamani Lakshminarayanan
Singapore Eye Research Institute
71 PUBLICATIONS **1,106** CITATIONS
SEE PROFILE

Xian Jun Loh
Agency for Science, Technology and Researc…
102 PUBLICATIONS **2,453** CITATIONS
SEE PROFILE

Yajnavalka Banerjee
Sultan Qaboos University
42 PUBLICATIONS **344** CITATIONS
SEE PROFILE

Suresh Valiyaveettil
National University of Singapore
232 PUBLICATIONS **6,655** CITATIONS
SEE PROFILE

Formation of Transient Amorphous Calcium Carbonate Precursor in Quail Eggshell Mineralization: An In Vitro Study

Rajamani Lakshminarayanan,[†,#] Xian Jun Loh,[†] Subramanyam Gayathri,[†] Swaminathan Sindhu,[‡] Yajnavalka Banerjee,[§] R. Manjunatha Kini,[§] and Suresh Valiyaveettil*[,†,‡]

Department of Chemistry, NUS−Nanoscience and Nanotechnology Initiative, and Department of Biological Sciences, National University of Singapore, Singapore, 3 Science Drive 3, Singapore 117543

Received June 7, 2006

To understand the mechanism of quail eggshell biomineralization, we have performed two $CaCO_3$ precipitation experiments. In the reprecipitation experiments, supersaturated $Ca(HCO_3)_2$ was prepared by bubbling CO_2 through a slurry of biogenic $CaCO_3$ obtained from bleach-treated eggshell followed by filtration to obtain a clear solution for crystallization experiments. The nucleated crystals were collected at various time intervals and analyzed. In the second experiment, the extracted SOM from the bleach-treated eggshell was added to the supersaturated clear solution of $Ca(HCO_3)_2$ solution obtained by bubbling CO_2 gas through a slurry of synthetic $CaCO_3$ followed by filtration. The crystals/precipitates collected at various time intervals were analyzed. Both experiments showed that amorphous $CaCO_3$ (ACC) was precipitated in the early stages, which then transformed to the most stable crystalline calcite phase. Amino acid analysis of the soluble organic matrixes (SOM) indicated the presence of high amounts of Glx and Asx amino acids. Ovomucoid—an acidic glycoprotein, and lysozyme—a basic protein, are the two major components along with a few low molecular weight peptides present in the SOM of quail eggshell matrix. Both ovomucoid and lysozyme did not induce precipitation of the ACC phase in in vitro conditions, while the fraction containing low molecular weight peptides induced the precipitation of ACC, suggesting that the latter play an important role in the eggshell biomineralization. Thus, organisms can produce inorganic minerals which assume nonequilibrium morphologies and intricate architecture by precipitating transient ACC, which then transformed into the crystalline phase. Altogether, these observations further demonstrate that this strategy may be common in both vertebrate and invertebrate mineralized structures.

Introduction

Avian eggshell consists of 95% inorganic mineral (calcite), along with an organic matrix. It acts as a potential facilitator for the exchange of gases and prevents the diffusion of water from contents of egg to the environment. A hen's eggshell contains about 7000−17000 pores, the density of which is inversely related to embryonic mortality.[1] The form and distribution of pores vary considerably among the avian species.[1b] In addition to variation in size, thickness, and the organization of mammillae, the soluble organic matrixes (SOM) of various domesticated species are also different among various birds.[2] Among the avian eggshells, SOM present in the chicken eggshells is the most extensively studied and is grouped into eggshell-specific proteins, egg white proteins, and bone matrix proteins. Ovocleidins (OC-17, OC-23, and OC-116) and ovocallyxins (OCX-32 and OCX-36) are the two classes of eggshell-specific proteins that have been extracted, purified, identified, and sequenced from chicken eggshells.[3] It is believed that these proteins are synthesized exclusively in the shell gland, where the calcification takes place in an extracellular milieu. Ansocalcin, a homologue protein of OC-17, has been identified and sequenced for the goose eggshell matrix.[4] OC-17 and ansocalcin belong to C-type lectin-like proteins (CTL). An interesting observation is the presence of two CTL proteins (struthiocalcin-1 and struthiocalcin-2) in ostrich eggshells, which showed high sequence identity to ansocalcin.[5] Emu and rhea eggshell matrixes also contain two CTL-like proteins, the complete amino acid sequences of which have been reported.[6]

Investigation of the mineral formation mechanism using a number of mineralized tissues has demonstrated that stereochemical complementarities exists between the organic matrix and the crystallographic orientation of mineral.[7] In certain marine invertebrates, a transient amorphous calcium carbonate (ACC), which transforms into a more stable polymorph, has been shown to be stabilized by specialized proteins.[8] The latter mechanism has also been demonstrated in vitro on two different animal phyla (echinoderms and mollusks).[9] The authors of these studies suggested that precipitation of ACC and its subsequent transformation to crystalline phase may be widespread in biology. Recently, the growth of ACC precursor phase in sea urchin spine and the association of ACC phase to the aragonitic region in mollusk shell have been demonstrated in vivo.[10]

Since eggshells are formed in an acellular environment at a rapid rate, it should be interesting to study whether the mineral formation is kinetically controlled or driven by complementary interaction between SOM and the mineral phase. Quail eggshells are interesting due to their small size as well as their pigmented nature. The strategy used here is to extract SOM from the eggshell matrix, purify, and identify the protein contents. Once the matrix proteins are identified, it is possible to compare across

* Corresponding author. E-mail: chmsv@nus.edu.sg.
† Department of Chemistry.
‡ NUS−Nanoscience and Nanotechnology Initiative.
§ Department of Biological Sciences.
# Present address: Center for Craniofacial and Molecular Biology, School of Dentistry, University of Southern California, 2250 Alcazar Street CSA 103, Los Angeles, CA 90033.

10.1021/bm0605412 CCC: $33.50
Published on Web 09/30/2006

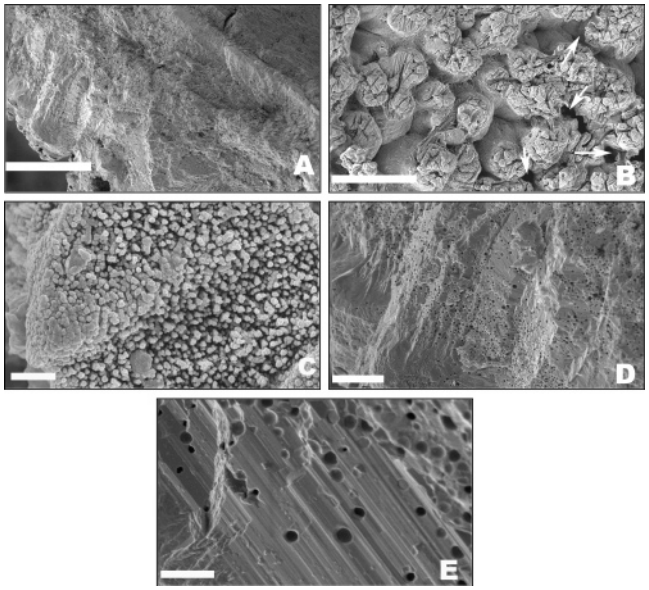

Figure 1. Electron micrographs of the calcified quail eggshells. (A) Cross section of the bleach-treated eggshell, scale bar = 100 μm. (B) Mammilary region, scale bar = 50 μm. The white arrow indicates the presence of large funnel-like pores. (C) Higher magnification of the mammilary layer indicating the assemblage of nanoparticles, scale bar = 500 nm. The white box in part B indicates the approximate location of the magnification. (D) Palisade region (scale bar = 10 μm). Note the presence of nanometer-sized pores randomly distributed throughout the mammilary and lower palisade layer. (E) Higher magnification of the palisade (scale bar = 2 μm). Note the presence of pores interspersed in the lamellar calcified layer.

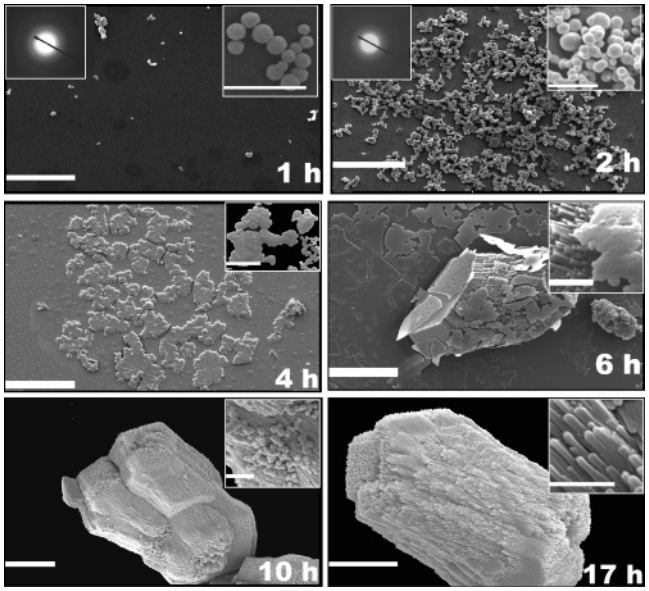

Figure 2. Representative electron micrographs of the $CaCO_3$ grown by the reprecipitation experiment at various time intervals. Scale bar = 10 μm; inset scale bar = 2 μm. The electron diffraction patterns shown at 1 and 2 h confirm the presence of ACC.

the avian family to see the similarities and differences in proteins involved in the eggshell mineralization. In vitro mineralization of $CaCO_3$ was investigated using two different experimental conditions, and the results are rationalized.

Results

Figure 1 shows the electron micrograph of various regions of the bleached quail eggshell. Unlike other avian eggshells, the mammilary layer of quail eggshell is much smaller in size and consists of disordered polycrystalline calcite aggregates (Figure 1B). Higher magnification of the aggregates in the mammilary layer indicates that this layer consists of closely assembled nanoparticles (Figure 1C). Since the mammilary layer is the first layer formed during eggshell formation, it is expected that these nanoparticles could act as anchoring units for the calcified shell on the shell membrane. The cross section of the shell further indicates that, in addition to the large pores, the mammilary and the lower palisade region of the shell consist of numerous nanopores/cavities (Figure 1D). Higher magnification images suggest that these pores are interspersed with isooriented nanorods of calcitic crystals (Figure 1E).

Reprecipitation Experiments Using Biogenic $CaCO_3$. It has been observed in all biomineralized structures that complete dissolution of the minerals by acids or a calcium chelator is required for extraction and purification of the biomacromolecules due to the intimate association between the biomacromolecules and the mineral phase. However, acidic conditions employed may cause deleterious effects on the biomacromolecules and use of calcium chelators is expected to alter the polarity by strongly binding to them.[7b,11] The strategy used here is to examine the formation of calcite phase without subjecting the biomacromolecules to such harsh treatments through a modified in vitro experiment. Briefly, the eggshells were treated with 5% hypochlorite bleach to remove the shell membrane. The remaining biogenic $CaCO_3$ powder was suspended in water (3 g/L), purified CO_2 was bubbled through this stirred suspension for 90 min, and the mixture was filtered using a 0.45 μm filter. To the resultant clear solution, CO_2 gas was bubbled again for 30 min to redissolve any traces of residual nuclei of $CaCO_3$ crystallites formed. The precipitation of mineral via the slow evaporation of this supersaturated calcium bicarbonate solution was monitored at various time intervals. This method is named as a reprecipitation experiment because the crystallization medium contains all soluble materials originally present in the eggshell matrix. Figure 2 shows the electron micrographs of $CaCO_3$ formed at various time intervals. A mesh of 400 $\pm$ 50 nm-sized spherical particles was formed on the microscopy slides within 1 h. These particles grew in size and formed larger particles of 700 $\pm$ 50 nm in diameter after 2 h. The submicrometer particles sintered together and formed a film-type structure that looked like a mosaic of polycrystalline patches in 4 h. No aragonite or vaterite phases have been observed within 2−4 h. After a 6 h period, well-ordered, lozenge-shaped calcite crystals were emerged from these patches. The surface of these crystals contained an array of microscopically aligned interdigitated calcite rods oriented along the *c*-axis that were reminiscent of the palisade layer. The crystals collected at 10 and 17 h were larger in size than the ones observed after 6 h, and no change in the morphology was observed. The mineralogy of the particles formed in the early stages (1 and 2 h) of the precipitation experiment was examined using selected area electron diffraction (SAED) experiments (inset, Figure 2). The appearance of diffuse rings in the SAED patterns supports the amorphous nature of the particles. FTIR spectra (Figure 3) of the precipitates formed after 1 and 2 h periods displayed splitting of the band at 1450 cm^{-1} (ν_3) and the presence of broad bands around 1068 cm^{-1} (ν_1) and 876 cm^{-1} (ν_2). These data along with the absence of the ν_4 absorption band at 713 cm^{-1} are characteristic of the ACC phase.[8] With increasing time of crystallization, the ν_1 band disappeared and a sharp peak at 713 cm^{-1} (ν_4) appeared representing the transition from ACC to the stable crystalline calcite phase. It is important to note that a

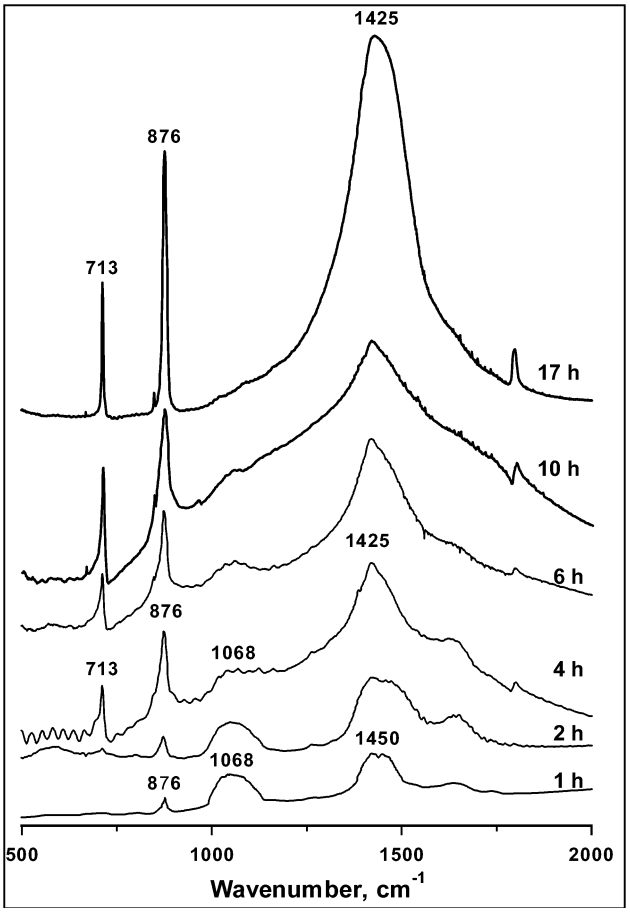

Figure 3. FTIR spectra of the $CaCO_3$ grown by the reprecipitation experiment at various time intervals. Note the progressive appearance of the ν_4 absorption peak at 713 cm^{-1}.

small amount of ACC is present even after 10 h of reprecipitation and the complete conversion to stable crystalline calcite phase only occurred after 17 h.

Influence of SOM on $CaCO_3$ Precipitation Using Commercial $CaCO_3$. The biogenic $CaCO_3$ contains inorganic ions such as magnesium, in addition to the SOM, which may influence the precipitation of ACC or nucleation of various polymorphs of $CaCO_3$. Therefore, SOM was extracted using acetic acid from the bleach-treated quail eggshells followed by microconcentration and lyophilization. The total content of the SOM was found to be 0.98 ± 0.03 wt %. The SOM (100 μg/mL) was then dissolved in supersaturated bicarbonate solution prepared by Kitano's procedure[12] using commercially available $CaCO_3$ powder, and the crystal growth experiments were performed as before at various time intervals (Figure 4). The precipitate collected was characterized by SEM, FTIR, and SAED techniques.

At 1 h, dumb-bell shaped structures of ca. 5 μm were formed on the glass plate. The surface of these structures consists of nanoparticles. These particles are larger than the particles observed in the early stage of reprecipitation experiments. The amorphous nature of particle was confirmed by the appearance of diffuse rings in the SAED pattern and the presence of characteristic ν_1 and absence of ν_4 IR absorption peaks (Figure 5). After 2 h, the particles maintained the dumb-bell shape and amorphous nature but the nanoparticles on the surface coalesced to form a sheath-type structure. At 4 h, two types of aggregates were observed—aggregates with a spherical shape and large hemispherical particles (minor amount). The surface of the spherical particles exhibits a terraced structure typical of a

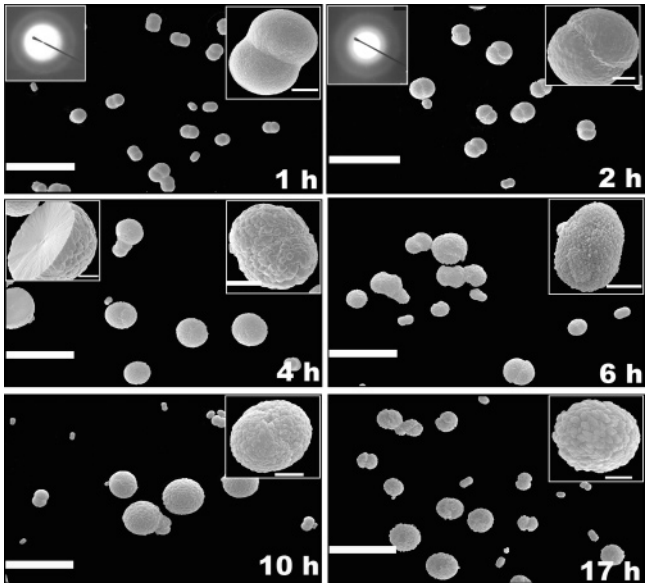

Figure 4. Representative electron micrographs of the $CaCO_3$ grown in the presence of SOM at various time intervals. Scale bar = 20 μm; inset scale bar = 2 μm. The electron diffraction patterns shown at 1 and 2 h confirm the presence of ACC.

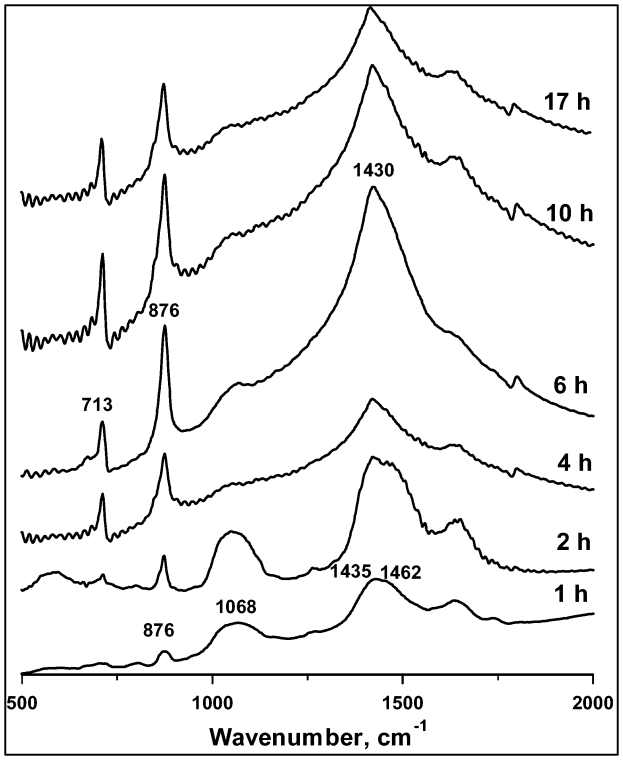

Figure 5. FTIR spectra of the $CaCO_3$ grown in the presence of SOM at various time intervals. Note the progressive appearance of the ν_4 absorption peak at 713 cm^{-1}.

crystalline phase. A closer examination of the hemispherical particles indicated tightly packed, uniformly aligned calcite crystallites capped with {104}-faces and may be formed as a result of radial outgrowth from the central region. The appearance of the 713 cm^{-1} peak in the IR spectrum indicates the transition from amorphous to crystalline calcite phase (Figure 5). As the time progressed, more and more polycrystalline calcite aggregates were formed. Thus, experiments performed in the presence of SOM suggest that ACC is precipitated in the early stages of eggshell biomineralization, and transformation to the thermodynamically more stable calcite phase begins after 2 h.

Table 1. Amino Acid Composition of the SOM Obtained from Bleach-Treated Quail Eggshell Extract

amino acid	composition mol %
Asx	13.59
Glx	12.07
Ser	7.23
Gly	9.87
His	2.81
Arg	4.60
Thr	7.63
Ala	5.31
Pro	6.37
Tyr	3.79
Val	8.57
Met	1.84
Ile	2.28
Leu	5.06
Phe	2.95
Lys	6.03

In the control experiments, regular rhombohedral crystals were nucleated during 1 and 2 h periods and no amorphous phase was observed (see the Supporting Information) further supporting that the SOM of quail eggshells induced the precipitation of ACC phase.

Analysis of the SOM. Amino acid analysis indicated that the extracted SOM was rich in Asx (13.59%) Glx (12.07%), and hydroxy (14.86%) amino acids (Table 1). SDS−PAGE of the SOM indicated the presence of biomacromolecules of various sizes (Figure 6A). The 30 kDa band was more intense compared to the 66 and 14 kDa bands and the low molecular weight bands. To identify the proteins corresponding to these bands, fractionation of the SOM was performed on a reversed-phase Jupiter C18 column (Figure 6B). The elution profile indicated a broad peak around 35% B as the major component. SDS−PAGE of this fraction (indicated by the horizontal line in the Figure 6B) showed a band around ∼30 kDa. The MALDI-TOF spectrum of the fraction yielded a broad distribution of masses ranging from 20 to 25 kDa, which is characteristic of a glycosylated protein (Figure 6C). Amino terminal sequence of this fraction, determined by Edman degradation of the first 37 residues is VEVDXSRFPX TTNEEGKDEV VXPDELRLIX GTDGVTY. No other additional peaks were observed during sequencing, which further confirms the homogeneity of this fraction. The amino terminal sequence corresponds to that of ovomucoid, an acidic glycoprotein (pI = 4.4), which is abundant in the egg white (∼11%).[13] Quail ovomucoid contains 186 amino acids with three tandem domains, each of which is homologous to pancreatic secretory trypsin inhibitor (Kazal type) and possesses putative reactive sites for the serine proteases. A large proportion of the carbohydrate present in this glycoprotein (about 11% w/w) was linked to the peptide backbone through the asparginyl residue and accounts for the relatively higher mass obtained by the SDS−PAGE compared to that from mass spectrometry. The fractions indicated by the horizontal dotted line in Figure 6B contain a number of low molecular weight peptides (see the Supporting Information). Partial amino terminal sequence of one of the peptides indicated the following sequence of amino acid residues—EAEEAQXEEV QAENNS. We were

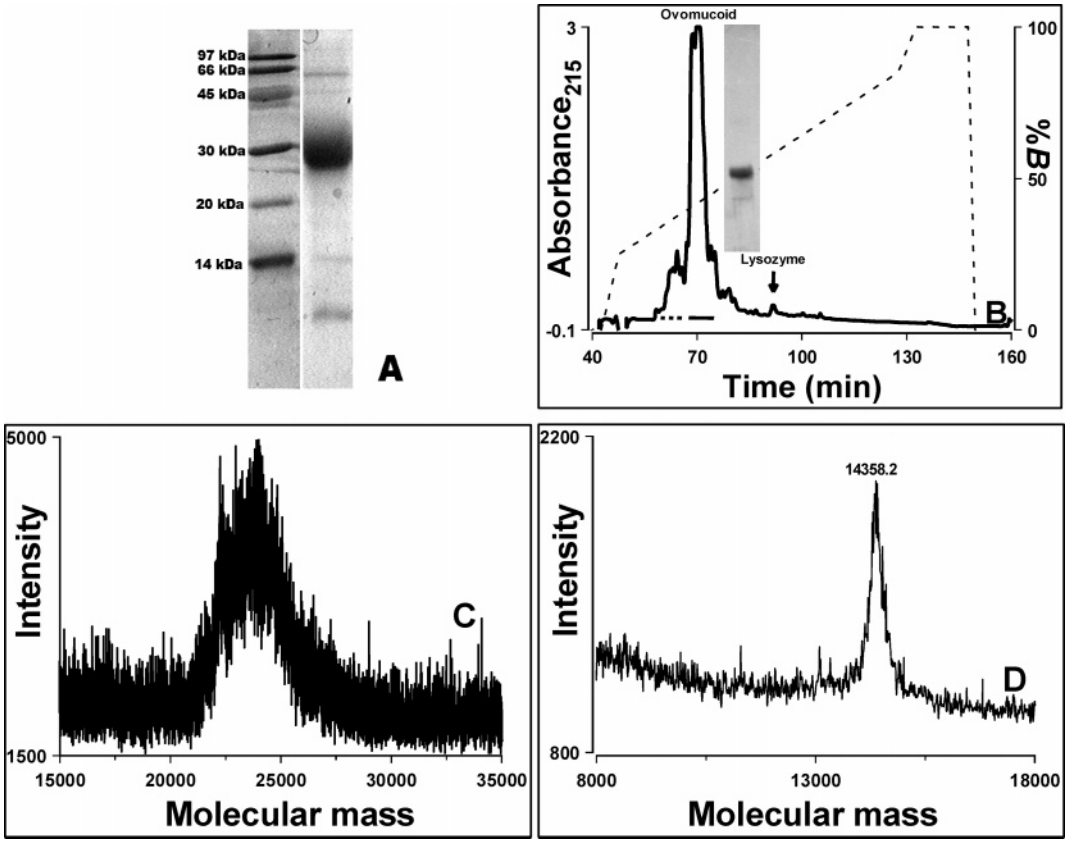

Figure 6. (A) SDS−PAGE of the SOM obtained from bleach-treated quail eggshell. (B) RP-HPLC profile of the SOM present in the bleach-treated quail eggshell. The elution position of ovomucoid is indicated by the solid horizontal line, and low molecular weight peptides are indicated by the dotted lines; 0.1% trifluoroacetic acid in 80% acetonitrile was used as the buffer B. The SDS−PAGE profile shown in the inset confirms the homogeneity of the ovomucoid (solid line). (C) MALDI-TOF mass spectrum of ovomucoid (the fraction indicated by the solid horizontal line in part B). (D) MALDI-TOF mass spectrum of lysozyme.

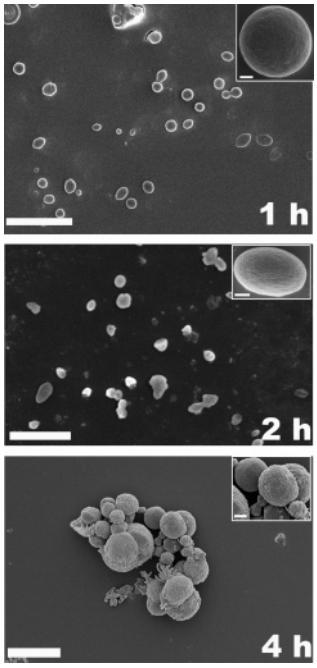

Figure 7. Representative electron micrographs of the $CaCO_3$ grown in the presence of low molecular weight peptides (pooled from the fractions indicated by the dotted horizontal line in Figure 6B). Scale bar = 5 μm; inset scale bar = 1 μm.

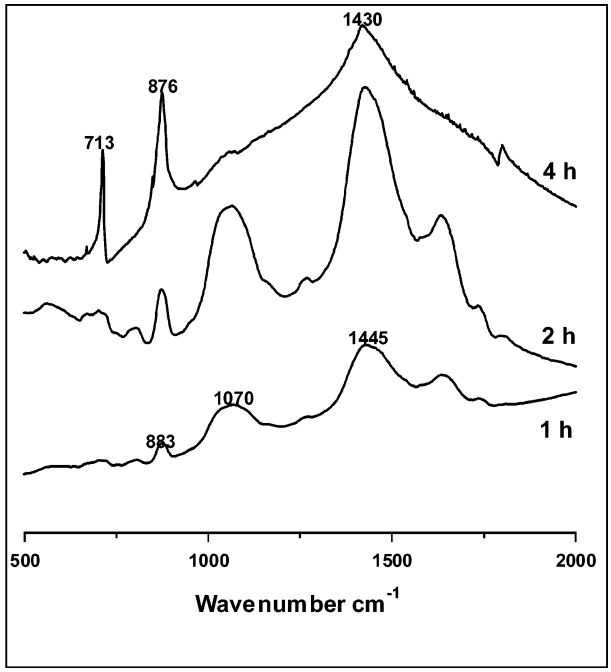

Figure 8. FTIR spectra of the $CaCO_3$ grown in the presence of low molecular weight fractions at various time intervals (pooled from the fractions indicated by the dotted horizontal line in Figure 6B).

not able to proceed further owing to the difficulty in isolating a significant quantity of these peptides for further purification. MALDI-TOF spectrum of the fraction that elutes around 55% B showed a mass of 14358.2 Da (Figure 6 D). The amino terminal sequence of the first eight amino acids (KVFGRXEL) corresponds to the sequence of lysozyme. Thus, ovomucoid and lysozyme are the two major components present in the bleach-treated quail eggshell, in addition to low molecular weight peptides.

Under in vitro environment, the proteins ovomucoid, lysozyme, and their 1:1 mixture (to check the activity of the mixture) did not induce the precipitation of the ACC phase. The nucleated crystals were similar to those observed in the control experiments. However, the pooled fractions with low molecular weight peptides (shown by the dotted horizontal line in the Figure 6B) induced the precipitation of the ACC phase (Figures 7 and 8) suggesting that these peptides play an important role in ACC precipitation.

Discussion

Morphologically, the cross section of eggshell has been described into various domains each of them exhibiting a different degree of orientation.[14] With the use of high-resolution electron microscopy, it is shown that the polycrystalline aggregates observed in the mammillary layer consist of closely assembled mineral nanoparticles (Figure 1). The palisade layer contains iso-oriented nanorods with interspersed pores/vesicles. Consistent with an earlier report, the high-resolution SEM images provide direct evidence for the presence of textural variations present on the quail eggshells.[14]

Eggshell fabrication begins in the red isthmus as the egg traverses the oviduct, and complete calcification takes place in the uterus in a highly temporal and sequentially controlled manner in the presence of an assembly of proteins.[15] The mineral deposition takes place in three stages viz., nucleation, growth, and inhibition of growth. It has been observed that the composition of uterus fluid, which contains many active matrix proteins, changes at each stage. Furthermore, the uterus fluid collected at these three stages has been shown to alter the kinetics and morphology of calcite crystals in vitro environments.[16] We believe that formation of the most stable phase, with specific crystallographic texture and meso/macrosopic porosity, in a short period of time requires a high activation energy. One plausible way to overcome this is through a sequential precipitation of the metastable phase(s). Since the initially formed phase would be the most soluble phase, a lower energy barrier is expected in accordance with the Ostwald−Lussac's law, which states that if the minerals exist in several polymorphic forms, then the most soluble ones precipitate first, while the least soluble precipitates last.[17] So far, transient ACC formation has been observed in marine invertebrates and is not seen in avian eggshell mineralization, either with whole SOM or purified/partially proteins.

Two different in vitro experiments were carried out to study if the calcite formation in eggshell is a one-step or multistep process. The results obtained by reprecipitation experiments indicate that mineralization takes place through the amorphous precursor phase. On the basis of the electron micrographs, it is clear that the initially formed ACC nanoparticles grew in size with time; a number of them consolidate forming clusters in 2 h. Sintering of these clusters resulted in randomly oriented partially crystalline patches within 4 h. FTIR spectra of these patches suggest a mixture of calcite and a significant amount of ACC (the IR spectra of the precipitate formed after 4 h in Figure 3 indicates a slight broadening of the ν_4 and the presence of a weak ν_1 absorption band, which are indicative of the existence of a mixture of ACC and calcite). With an increase in time, lozenges-type crystals emerge from these mosaic patches. The surface of these crystals contains uniformly aligned nanorods. A possible explanation for this could be that the ACC domain present in the precursor polycrystalline patches dissolves and recrystallizes on the seed crystals producing lozenges-shaped crystals. Although, it is difficult to explain the transformation from film to lozenge-shaped crystals, it is likely that the

formation of mosaic patches follows a similar mechanism involving highly acidic macromolecules.[18] Since these patches contain both ACC and crystalline calcite crystals, formation of lozenge-shaped crystals is directed by the seed crystals. It has been shown that "seed crystals" act as the template for crystallographic orientation of the sea urchin spines.[19] Elemental analysis of the bleach-treated eggshells indicates a magnesium content of 2.1 ± 0.2 mol %. Since the presence of magnesium ions influences the "liquid precursor phase", it is conceivable that the lozenges-shaped crystals were formed through a biopolymer-induced liquid precursor (bioPILP) process.[20] The dissolution of biogenic $CaCO_3$ releases intracrystalline SOM and other ions into the solution, which increases the local supersaturation through (non)specific binding of the calcium ions and resulted in the precipitation of the ACC phase. Thus, the reprecipitation method can be used as a "rapid check" to study the characteristics of the mineralization process. The absence of extreme pH and denaturing conditions in the procedures is also an added advantage of this method. However, the presence of trace amounts of other inorganic ions may influence the reprecipitation process. Therefore, an independent experiment should be performed to understand the role of SOM.

The formation of ACC in the presence of SOM indicates that calcite crystallization is preceded by the ACC precipitation. Since no inorganic ions were added in the crystallization medium, only the influence of SOM in the precipitation of ACC is established. Unlike the reprecipitation experiments, the dumbbell ACC particles formed in the early stages transformed into spherical/ellipsoidal polycrystalline calcite aggregates without undergoing large deformation in shape. It is likely that in the amorphous phase the ions are irregularly arranged owing to the presence of varying degrees of hydration; transformation of ACC to the more stable crystalline phase (less soluble) occurs through the expulsion of water as the mineral assumes a lower energy state. This difference in the transformation mechanism could be due to the presence of other "impurities" such as low molecular weight inorganic ions in the biogenic $CaCO_3$ or due to different concentrations of SOM.

Despite these differences, both methods indicate that eggshell biomineralization is a two-step process, i.e., precipitation of the transient ACC, which subsequently transforms to the thermodynamically stable calcite phase given the conditions that the temporal modifications in crystallization kinetics is prevalent in avian eggshells.[17] It is likely that by precipitating the ACC phase, the matrix proteins could choose to manipulate the orientation and porosity of the eggshell to meet specific biological functions.

$CaCO_3$ exists in three crystalline modifications: calcite, aragonite, and vaterite. Aragonite and calcite are abundant, while metastable vaterite phase is rare in natural systems. Aragonite and vaterite phases are metastable with respect to calcite by an order of few kJ/mol, and at a given temperature the metastability is governed by the enthalpy (ΔH) term.[21] The order of thermodynamic stability can be easily reversed by controlling the particle size, and therefore, by precipitating the ACC nanoparticles in the early stages, organisms surmount the large free energy required for the crystallization of thermodynamically stable polymorph. Since ions present in the amorphous particles have loosely packed structures, they may be able to relax readily by rotating/changing the bond angles and bond lengths contrary to solid-state transformation. Such a stress relaxation mechanism has been hypothesized in the biomimetic formation of large calcite single crystals.[22] The observation of nanoparticles in the mammilary layer of the eggshell further supports our idea that ACC nanoparticles could be formed in the early stages of eggshell calcification.

It has been observed that specialized macromolecules occluded in the crystal lattice of many calcite skeletal tissues altered the fracture mechanics.[7b] The total SOM present in the bleach-treated eggshell was found to be 0.98 ± 0.03 wt %. Amino acid analysis of SOM indicated that it is rich in Asx, Glx, Gly, and hydroxy amino acids. A similar composition was observed in the case of macromolecules extracted in the early stage of spicule, *Strongylocentrotus purpuratus*.[8g] Fractionation of the SOM on a reversed-phase column indicated the presence of ovomucoid, lysozyme, and a number of low molecular weight peptides as the components. Earlier studies have shown that ovotransferrin, ovalbumin, lysozyme, and clusterin are the egg white proteins identified in the chicken eggshells.[23] Since bleach treatment removes shell membrane and other proteins externally associated with the mineral phase, ovomucoid, lysozyme, and the low molecular weight peptides are present as an intracrystalline component. Presence of Glu-rich peptide also suggests that they may have a significant role in the precipitation of the ACC phase. Such Glu-rich protein has been isolated from the cuticles of the penaeid prawn.[24] The absence of ovocleidin-type proteins and the presence of ovomucoid as the major component are the distinct features observed in the SOM of quail eggshells.

When the crystal growth experiment was performed in the presence of ovomucoid, lysozyme, and their 1:1 mixture, no ACC precipitation was observed highlighting the importance of other components. However, in a separate experiment the fractions containing low molecular weight peptides from SOM induced the ACC phase. Owing to the low abundance, obtaining significant quantity of the homogeneous peptides from SOM remains a daunting task at present. Moreover, it is difficult to understand the reason for the high abundance of ovomucoid in the bleached eggshells; it may function as an enzyme inhibitor or interact/moderate the activities of peptides in the quail eggshell matrix.

Stable ACC has been shown to be an integral component in a number of marine animals such as Ascidiacea and Crustacea.[8f,25] The stabilization of ACC may be determined by the amount of Mg^{2+} or phosphate ions or specialized biomacromolecules present in the skeleton. Transient ACC-bearing skeletons contain <5 mol % magnesium in the crystal lattice, and the presence of 2.1 mol % magnesium in quail eggshells complies with these results. Although it is difficult to account for the advantages gained by an organism in precipitating the ACC phase, it is possible that the organism utilizes the ACC precursor phase to mold the most stable crystalline phase best suited to its requirements. This is the first report on the formation of transient ACC by SOM of $CaCO_3$ vertebrate (avian eggshells) and may imply that phylogenetically unrelated organisms (e.g., marine invertebrates such as sea urchin or mollusks) have adopted a strikingly similar strategy for the biomineralization process.

Conclusions

The results presented in this paper highlight two important aspects of biomineralization in quail eggshell matrix: (i) the transient formation of ACC and its subsequent transformation to a stable crystalline phase is widespread within the invertebrates, and the results obtained demonstrate that this transformation can also occur in vertebrates, and (ii) the presence of low molecular weight peptides has a profound influence on the ACC phase. Overall, despite an overwhelming similarity in the structure and functional nature of avian eggshells, their miner-

alization is controlled by distinctly different groups of proteins. A comparative study of other avian eggshells using the methodology reported here would improve our understanding of eggshell mineralization.

Experimental Section

Reprecipitation and Characterization of Biogenic $CaCO_3$. Fresh eggs purchased from the market were crack-opened and washed extensively with running water and then with MilliQ water for about 30 min to remove the yolk and egg white. Powdered eggshells were bleached with sodium hypochlorite solution (5%) for about 15 min to remove traces of the shell membrane or extrashell organic materials, washed extensively with water to remove the residual bleach, and air-dried at room-temperature overnight. Elemental analyses of the samples were carried out using a Thermo Jarrel Ash Duo Axis Plasma model ICP−OES. The standards (Ca^{2+} concentrations of 1−10 ppm, Mg^{2+} concentrations of 0.1−1 ppm) for calibration were prepared using stock solution of calcium nitrate (1000 ppm, BDH Laboratory Supplies, England) and magnesium nitrate solution (1000 ppm, Alpha Analytical-(S) Pte Ltd). The elemental content of the sample was analyzed using 0.1 mg of the bleach-treated eggshell powder, digested in concentrated HCl and appropriately diluted for analyses. Triplicate analyses were performed, and average values are reported.

The powdered eggshell was suspended in MilliQ water and stirred (3 g/L). To the stirred suspension, purified CO_2 gas was passed for 90 min, filtered using a 0.45 m filter, and CO_2 gas was bubbled through the solution for 30 min. Typically, 1 mL of this solution was placed on a 12 mm coverslip kept in a 3 cm Petridish covered with aluminum foil with a few pinholes. The precipitate obtained at various time intervals was characterized using electron microscopy and FTIR spectroscopy after rinsing with water and air-drying. The morphology of $CaCO_3$ was examined using Phillips XL 30 FEG scanning electron microscope at 5/10 kV after sputter coating with gold to increase the conductivity. For the electron diffraction (ED) experiments, the precipitate was collected on a Formvar-coated Cu grid, rinsed gently with water, and air-dried. The ED pattern was recorded on a JEOL 2010 electron microscope. IR analyses of the sample were performed using a Bio-Rad FTIR spectrometer at 4 cm^{-1} resolution. A powdered sample of the precipitate was made into a pellet after mixing with anhydrous KBr and used for IR analyses.

Influence of SOM on $CaCO_3$ Precipitation Using Commercial $CaCO_3$. Supersaturated $Ca(HCO_3)_2$ solution was prepared by using commercial $CaCO_3$ (3 g/L) as reported earlier for the biogenic $CaCO_3$. The pH of the solution was 6.1. SOM, lysozyme, ovomucoid, and the partially purified peptides (100 μg/mL) were dissolved in this solution; the precipitation and characterization experiments were carried out as before.[12]

Extraction of SOM. The bleach-treated eggshells were digested with 30% acetic acid at 4 °C overnight so that the final pH remains above 4. About 400 mL of this solution was concentrated to 40 mL on an Amicon microconcentrator using a YM1 (1000 MW cutoff) membrane filter. MilliQ water was added to the concentrated suspension, and the turbid solution was concentrated again. The procedure was repeated twice to ensure complete removal of inorganic ions and other low molecular weight compounds. The resultant turbid solution was centrifuged at 4000 rpm at 4 °C, and the centrifugate was lyophilized. The amount of SOM has been found to be 0.98 ± 0.03 wt % and was used for purification and in vitro precipitation experiments. SDS−PAGE of SOM was performed on 15% gel under nonreducing conditions. The amino acid composition of the bleach-treated eggshell extract was determined by the hydrolysis of 300 μg of the sample in 6 N HCl in vacuo at 110 °C for 24 h. The hydrolyzed products after evaporation of HCl were separated on a Pico-tag column (3.9 mm × 15 cm), postcolumn derivatization was done with phenyl isothiocyanate, and the derivatized products were detected at 254 nm using a Waters 2487 dual wavelength absorbance detector at the Advanced Protein Technology Centre, Hospital for Sick Children, Toronto, Canada.

Identification and Characterization of Matrix Proteins. The SOM was dissolved in 10 mM $CaCl_2$ solution and fractionated on a Jupiter C18 reversed-phase column (5 μm, 250 mm × 10 mm) using a Vision workstation (Perkin-Elmer PerSeptive Biosystems). The column was equilibrated with 0.1% trifluoroacetic acid, and the bound proteins were eluted using a linear gradient of buffer B (0.1% TFA in 80% acetonitrile) at a flow rate of 2 mL/min. Elution of the various fractions was monitored at 215 and 280 nm. Fractions which contained the ovomucoid (indicated by the horizontal line in Figure 6B) were pooled and lyophilized for further studies. MALDI-TOF of the ovomucoid was obtained on a Voyager-DE Biospectrometry workstation equipped with a 337 nm nitrogen laser. To obtain a good signal-to-noise ratio, 150−200 single-shot spectra were collected. Saturated sinapinic acid in 50% acetonitrile was used as the matrix. The fraction (0.5 μL) was mixed with 0.5 μL of the matrix and dried on a 96 × 2 sample holder prior to the analysis. Amino terminal sequencing of the native fraction was performed by the automated Edman degradation method using a Perkin-Elmer Applied Biosystems 494 pulsed-liquid-phase protein sequencer (Procise) with an online 785A PTH−amino acid analyzer.

Acknowledgment. R.L.N. thanks the Singapore Millennium Foundation for the award of a fellowship. X.J.L. thanks the Agency for Science, Technology and Research (ASTAR) for the award of the BS−PhD scholarship, S.V. acknowledges the National University of Singapore (NUS) for a research scholarship, S.S. thanks the NUS−Nanoscience and Nanotechnology Initiative (NUSNNI) for a research fellowship, and S.V. acknowledges the funding support from the NUS and ASTAR.

Supporting Information Available. Additional figures and peptide analysis. This material is available free of charge via the Internet at http://pubs.acs.org.

References and Notes

(1) Peebles, E. D.; Brake, J. *Poult. Sci.* **1985**, *64*, 2385. (b) Board, R. G.; Tullet, S. G.; Perrott, H. R. *J. Zool.* **1977**, *251*, 1982.
(2) Panheleux, M.; Bain, M.; Fernandez, M. S.; Morales, I.; Gautron, J.; Arias, J. L.; Solomon, S. E.; Hincke, M. T.; Nys, Y. *Br. Poult. Sci.* **1999**, *40*, 240.
(3) Hincke, M. T.; Tsang, C. P. W.; Courtney, M.; Hill, V.; Narbaitz, R. *Calcif. Tissue Int.* **1995**, *56*, 578. (b) Mann, K.; Siedler, F. *Biochem. Mol. Biol. Int.* **1999**, *47*, 997. (c) Mann, K. *FEBS Lett*. **1999**, *463*, 12. (d) Gautron, J.; Hincke, M. T.; Mann, K.; Panheleux, M.; McKee, M. D.; Bain, M.; Solomon, S. E.; Nys, Y. *J. Biol. Chem.* **2001**, *276*, 39243. (e) Hincke, M. T.; Gautron, J.; Mann, K.; Panheleux, M.; Bain, M.; McKee, M. D.; Solomon, S. E.; Nys, Y. *Connect. Tissue Res.* **2003**, *44*, 16.
(4) Lakshminarayanan, R.; Valiyaveettil, S.; Rao, V. S.; Kini, R. M. *J. Biol. Chem.* **2003**, *278*, 2928.
(5) Mann, K.; Siedler, F. *Biochim. Biophys. Acta: Proteins Proteom*. **2004**, *1626*, 41.
(6) Mann, K. *Br. Poult. Sci.* **2004**, *45*, 483. (b) Mann, K.; Siedler, F. *Comp. Biochem. Physiol. B* **2006**, *143*, 160.
(7) Fritz, M.; Belcher, A. M.; Radmacher, M.; Walters, D. A.; Hansma, P. K.; Stucky, G. D.; Morse D. E. *Nature* **1994**, *371*, 49. (b) Albeck, S.; Aizenberg, J.; Addadi, L.; Weiner, S. *J. Am. Chem. Soc*. **1993**, *115*, 11691.
(8) Aizenberg, J.; Lambert, G.; Addadi, L.; Weiner, S. *Adv. Mater*. **1996**, *8*, 222. (b) Beniash, E.; Aizenberg, J.; Addadi, L.; Weiner, S. *Proc. R. Soc. London, Ser. B* **1997**, *264*, 461. (c) Beniash, E.; Addadi, L.; Weiner, S. *J. Struct. Biol*. **1999**, *125*, 50. (d) Raz, S.; Weiner, S.; Addadi, L. *Adv. Mater*. **2000**, *12*, 38. (e) Aizenberg, J.; Lambert, G.; Weiner, S.; Addadi, L. *J. Am. Chem. Soc*. **2002**, *124*, 32. (f) Aizenberg, J.; Weiner, S.; Addadi, L. *Connect. Tissue Res*. **2003**, *44*, 20. (g) Raz, S.; Hamilton, P. C.; Wilt, F. H.; Weiner, S. Addadi, L. *Adv. Funct. Mater*. **2003**, *13*, 480. (h) Weiss, I. M.; Tuross, N.; Addadi, L.; Weiner, S. *J. Exp. Zool*. **2002**, *293*, 478. (i) Hasse, B.; Ehrenberg, H.; Marxen, J. C.; Becker, W.; Epple, M. *Chem.—Eur. J*. **2000**, *6*, 3679. (j) Gotliv, B. A.; Addadi, L.; Weiner, S. *ChemBioChem* **2003**, *4*, 522.
(9) Addadi, L.; Raz, S.; Weiner, S. *Adv. Mater*. **2003**, *15*, 959.
(10) Politi, Y.; Arad, T.; Klein, E.; Weiner, S.; Addadi, L. *Science* **2004**, *306*, 1161. (b) Nassif, N.; Pinna, N.; Gehrke, N.; Antonietti, M.; Jager, C.; Colfen, H. *Proc. Natl. Acad. Sci., U.S.A.* **2005**, *102*, 12653.

(11) Wheeler, A. P.; Rusenko, K. W.; George, J. W.; Sikes, C. S. *Comp. Biochem. Physiol. B* **1987**, *87*, 953.
(12) Kitano, Y. *Bull. Chem. Soc. Jpn.* **1962**, *35*, 1973.
(13) Awade, A. C. *Z. Lebensm Unters Forsch A.* **1996**, *202*, 1. (b) Hase, S.; Okawa, K.; Ikenaka, T. *J. Biochem.* **1982**, *91*, 735.
(14) Lammie, D.; Bain, M. M.; Wess, T. J. *J. Synchrotron Radiat.* **2005**, *12*, 721.
(15) Fernandez, M. S.; Moya, A.; Lopez, L.; Arias, J. L. *Matrix Biol.* **2001**, *19*, 793. (b) Gautron, J.; Hincke, M. T.; Nys, Y. *Connect. Tissue Res.* **1997**, *36*, 195.
(16) Dominguez-Vera, J. M.; Gautron, J.; Garcia-Ruiz, J. M.; Nys, Y. *Poult. Sci.* **2000**, *79*, 901. (b) Gautron, J.; Hincke, M. T.; Nys, Y. *Connect. Tissue Res.* **1997**, *36*, 195.
(17) Leadbeater, B., Riding, R., Eds. *Biomineralization in Lower Plants and Animals*; Clarendon Press: New York, 1986.
(18) Gower, L. A.; Tirrel, D. A. *J. Cryst. Growth* **1998**, *191*, 153. (b) Olszta, M. J.; Odom, D. J.; Douglas, E. P.; Gower L. B. *Connect. Tissue Res.* **2003**, *44*, 326.
(19) Wilt, F. H. *J. Struct. Biol.* **1999**, *126*, 216.
(20) Olszta, M. J.; Gajjeraman, S.; Kaufman, M.; Gower, L. B. *Chem. Mater.* **2004**, *16*, 2355.
(21) Navrotsky, A. *Proc. Natl. Acad. Sci. U.S.A.* **2004**, *101*, 12101.
(22) Aizenberg, J.; Muller, D. A.; Grazul, J. A.; Hamann, D. R. *Science* **2003**, *299*, 1205.
(23) Nys, Y.; Gautron, J.; McKee, M. D.; Garcia-Ruiz, J. M.; Hincke, M. T. *World Poult. Sci. J.* **2001**, *57*, 401. (b) Mann, K.; Gautron, J.; McKee, M. D.; Bajari, T.; Schneider, W. J.; Hincke, M. T. *Matrix Biol.* **2003**, *22*, 397.
(24) Endo, H.; Takagi, Y.; Ozaki, N.; Kogure, T.; Watanabe, T. *Biochem. J.* **2004**, *384*, 159.
(25) Becker, A.; Ziegler, A.; Epple, M. *J. Chem. Soc., Dalton Trans.* **2005**, 1814. (b) Raz, S.; Testenière, O.; Hecker, A.; Weiner, S.; Luquet, G. *Biol. Bull.* **2002**, *203*, 269. (c) Dillaman, R.; Hequembourg, S.; Gay, M. *J. Morphol.* **2005**, *263*, 356.

BM0605412